Pergamon

Int. J. Solids Structures Vol. 32, No. 5, pp. 629–645, 1995

0020–7683/95 $9.50 + .00

0020–7683(94)00103–0

BOUNDARY LAYERS IN WEDGES OF LAMINATED COMPOSITE STRIPS UNDER GENERALIZED PLANE DEFORMATION–PART II: COMPLETE NUMERICAL SOLUTIONS

TAE WOAN KIM and SEYOUNG IM
Department of Mechanical Engineering, Korea Advanced Institute of Science and Technology, Science Town, Taejon 305-701, Korea

(*Received* 29 *October* 1993; *in revised form* 28 *May* 1994)

Abstract—A procedure for finding complete numerical solutions for the elastic boundary layer field in wedges of a laminated composite strip under the generic loadings of generalized plane deformation is discussed together with numerical examples for free edge problems and delamination crack problems. The procedure yields the solution in terms of loading parameters and is applicable to an arbitrary wedge angle and ply orientation and any type of loadings within the range of generalized plane deformation. For the free edge problem, the so called free edge stress intensity and the mode vector are defined and the free edge stress intensity is found to be a single parameter governing the fracture or failure behaviour near the free edge for a given pair of adjacent materials (plies). The effect of relative ply thickness upon the stress intensity and the energy release rate is also discussed for various types of loadings.

1. INTRODUCTION

The boundary layer problems for wedges on the cross-section of a laminated composite strip have been subjects under intensive investigation for the last two decades: particularly among others are the free edge problems [see Wang and Choi (1982); Zwiers *et al.* (1984) and papers cited therein] and the delamination crack problems (Wang, 1984) in the field of mechanics of composite materials. The structure of this boundary layer solution has been obtained in Part I of this paper (Kim and Im, 1994) for all wedge angles and for an arbitrary pair of ply orientations under the generic loadings of the so called generalized plane deformation. The nature of the asymptotic field has been discussed together with the possibility of existence of a logarithmic eigenfunction like the term $z_k \ln z_k$ for various loading conditions.

In this paper, we are concerned with the complete numerical solution for the boundary layers on the wedge type cross-section of a laminated composite strip under generic loadings of generalized plane deformation, such as tension, pure bending and/or torsion. A special singular hybrid finite element method, wherein the asymptotic eigensolution obtained in Part I of this paper is embedded, is combined with displacement based finite elements. These elements surround the hybrid finite element to model the far field region on the cross-section of a strip. It is also shown that the solution is obtained in terms of the loading parameters via the end conditions or via the expressions for force and moment resultants, not in terms of deformation parameters.

The asymptotic solutions are briefly summarized in Section 2. In Section 3, the singular hybrid finite element method is formulated together with a concise description about contact treatment, which is useful for treating closed delamination cracks. The procedure of converting the solution in terms of deformation parameters into in terms of loading parameters is discussed next. Numerical examples in Section 4 include the free edge problems and the delamination crack problems. The convergence of numerical solution is examined in terms of the total number of eigenfunction terms embedded in the hybrid element. Moreover, the effect of the ply thickness upon the resulting stress intensity is examined. For free edge problems, the so called free edge stress intensity and mode vector are defined to characterize the singular traction vector on the interface near the free edge for a given

pair of adjacent materials. The free edge stress intensity is found to be a single scaling parameter needed to represent the stress state near the free edge, regardless of the type of applied loadings, for a given pair of adjacent materials. For the delamination crack problems, wherein the crack faces may be opened or closed, either hybrid element of opened crack model or closed crack model is chosen based upon the results from the regular finite element analysis. The numerical results are obtained in terms of Suo's stress intensity factors and the energy release rate.

2. ASYMPTOTIC SOLUTIONS

When a laminated composite strip having a wedge type cross-section is subjected to generalized plane deformations, which include the generalized plane strain deformations and a class of deformations arising from the end loadings with no shear force, such as tension/compression, bending and/or torsion, a boundary layer region is developed near the tip of a wedge due to geometric and material discontinuity. Such types of problems include the well known free edge and delamination problems. The asymptotic solution structure for the displacements and stresses for the boundary layer near a wedge of such a laminated composite strip may be obtained from appropriate near field conditions (Kim and Im, 1994). In the absence of logarithmic eigenfunctions in homogeneous solutions, which is the case in general for free edges and delamination cracks in laminated composites, the asymptotic form of homogeneous solutions for the displacements and stresses are given by eqns (17e) in Part I (Kim and Im, 1994). The unknown β_ns of eqns (17e) in Part I are real constants to be determined in conjunction with a particular solution through remote boundary conditions. Generally, there are an infinite number of eigenvalues δ_n so that the number of unknown constant β_ns is infinite. Proper truncation of the infinite eigenfunction series is needed in order to approximate the boundary layer solutions.

For the aforementioned generalized plane deformation of a laminated composite strip with a wedge type cross-section, Kim and Im (1994) have shown that the particular solutions for stress and displacement may include logarithmic functions in addition to polynomial functions. These particular solutions for stresses and displacements are given by eqns (22a,b) or (27a,b) in Part I (Kim and Im, 1994). The complete solution for the boundary layer region in a wedge shaped discontinuity on the cross-section of a laminated composite strip comprises the homogeneous solution and the particular solution in question.

3. FINITE ELEMENT SOLUTION PROCEDURE

In this section, we discuss how to determine the unknown constants γ_{kn} or β_n in the asymptotic solutions for stresses and displacements (see eqns 17a–e in Part I; Kim and Im, 1994). To complete the solution, we need to determine these unknown constants from the far field boundary conditions and the end conditions. The cases of plane strain problems or of generalized plane deformation problems in terms of deformation parameters $A_i (i = 1\text{–}4)$ do not involve any end conditions prescribed in terms of axial force, bending moment and/or torsion. We have only to match the asymptotic solution with the far field conditions in the remote boundary via suitable numerical techniques such as the boundary collocation technique (Kim and Im, 1991), the enriched finite element method (Stolarski and Chiang, 1989; Atluri *et al.*, 1986) or the singular hybrid finite element method (Wang and Yuan, 1983 or Kim and Im, 1993). For the present problem, wherein the loading is prescribed in terms of axial force and/or moments, with all four deformation parameters A_i possibly non-zero, on the end of a laminated composite strip, we need to impose the end conditions for obtaining the solution. This procedure enables us to convert the solution in terms of deformation parameters into the solution in terms of end force and/or end moments, regardless of the ply orientations and regardless of the type of loadings within the range of generalized plane deformations.

In this work, we rely upon the singular hybrid finite element technique. The essence of this scheme is that the asymptotic solutions truncated properly is embedded into the hybrid element so that the near field is matched with the remote field represented by the surrounding

regular elements. In the present problem where the loading conditions on the ends are to be imposed, the hybrid FEM has a definite advantage over the boundary collocation technique (Kim and Im, 1993) in the aspect of integrating the traction for calculating the resultant loadings on the cross section.

3.1. *Formulation of the singular hybrid element*

To illustrate the basic scheme of stiffness matrix formulation for the singular composite wedge element, we consider a laminated composite subjected to generic loadings of a generalized plane deformation. The stiffness matrix of singular element in the case of general three-dimensional deformations is formulated on the basis of the modified hybrid variational functional $\pi_{mh}(\boldsymbol{\sigma}, \mathbf{u}, \bar{\mathbf{u}}, \mathbf{T})$ in Washizu (1988):

$$\pi_{mh}(\boldsymbol{\sigma}, \mathbf{u}, \bar{\mathbf{u}}, \mathbf{T}) = \int\int_{\Omega_m} (\boldsymbol{\sigma}^T\boldsymbol{\varepsilon} - \tfrac{1}{2}\boldsymbol{\sigma}^T\mathbf{S}\boldsymbol{\sigma})\, \mathrm{d}V - \int_{\partial\Omega_m} \mathbf{T}^T(\mathbf{u}-\bar{\mathbf{u}})\, \mathrm{d}A - \int_{S_{\sigma_m}} \mathbf{T}^{*T}\bar{\mathbf{u}}\, \mathrm{d}A, \tag{1}$$

where Ω_m is the volume of the m-th singular hybrid element; $\partial\Omega_m$ is the boundary of Ω_m; S_{σ_m} is the portion of element boundary $\partial\Omega_m$ where traction $\mathbf{T}^*$ is prescribed; and $\bar{\mathbf{u}}$ is a displacement vector defined along the singular element boundary. Standard matrix notation $\mathbf{S}, \boldsymbol{\sigma}, \boldsymbol{\varepsilon}, \mathbf{u}$ and $\mathbf{T}$ in the finite element analysis are used here for convenience to represent the compliance matrices, stresses, strains and displacements in the interior of the element, and tractions along the boundary, respectively. Taking variation of the functional (1), we can find that the Euler equations are given by

$$\boldsymbol{\varepsilon} = \mathbf{S}\boldsymbol{\sigma} \quad \text{and} \quad \mathbf{D}\boldsymbol{\sigma} = 0 \quad \text{in} \quad \Omega_m, \tag{2a}$$

$$\mathbf{T} = \mathbf{n}\boldsymbol{\sigma} \quad \text{and} \quad \mathbf{u} = \bar{\mathbf{u}} \quad \text{on} \quad \partial\Omega_m, \tag{2b}$$

$$\mathbf{T} = \mathbf{T}^* \quad \text{on} \quad S_{\sigma_m}, \tag{2c}$$

where $\mathbf{D}$ is the matrix operator for equilibrium equation. The hybrid finite element approach requires that the asymptotic solutions for stress and displacement, $\boldsymbol{\sigma}$ and $\mathbf{u}$ within the element and the boundary displacement, $\bar{\mathbf{u}}$ be assumed independently, and in case all of the Euler equations, except for the second in eqn (2b), are satisfied exactly for the generalized plane deformations, the functional π_{mh} reduces to

$$\pi_{mh}(\mathbf{U}, \bar{\mathbf{U}}) = \int_{\partial A_m} \mathbf{T}^T\bar{\mathbf{U}}\, \mathrm{d}s - \frac{1}{2}\int_{\partial A_m} \mathbf{T}^T\mathbf{U}\, \mathrm{d}s - \frac{1}{2}\int\int_{A_m} \boldsymbol{\sigma}^T\boldsymbol{\varepsilon}^A\, \mathrm{d}A, \tag{3}$$

in the absence of traction on S_{σ_m}, where $\mathbf{U}$ and $\bar{\mathbf{U}}$ are the displacements of eqn (4) in Part I (Kim and Im, 1994) and they are defined on the area of the m-th singular element A_m and along its boundary ∂A_m, respectively; $\boldsymbol{\varepsilon}_A$ is the strain resulting from $\mathbf{u}_A$ and is given as $(0, 0, A_1 + A_2x_1 + A_3x_2, A_4x_1, -A_4x_2, 0)^T$ and $\mathbf{T}$ and $\boldsymbol{\sigma}$ are the traction and stress resulting from $\mathbf{U}$, respectively.

Since the asymptotic solution structure for a wedge type cross section of a laminated composite strip subjected to the aforementioned loadings of generalized plane deformation has been determined explicitly in the previous section, we can immediately establish expressions for $\boldsymbol{\sigma}$ and $\mathbf{U}$ in the hybrid element. Matrix forms for $\boldsymbol{\sigma}$, $\mathbf{T}$ and $\mathbf{U}$ can be written as

$$\boldsymbol{\sigma} = \mathbf{P}\boldsymbol{\beta} + \boldsymbol{\sigma}^p, \mathbf{T} = \mathbf{R}\boldsymbol{\beta} + \mathbf{T}^p, \mathbf{U} = \underline{\mathbf{U}}\boldsymbol{\beta} + \mathbf{U}^p, \tag{4}$$

where $\boldsymbol{\beta}$ are unknown real parameters, and $\boldsymbol{\sigma}^p$, $\mathbf{T}^p$ and $\mathbf{U}^p$ are known quantities resulting from the particular solutions. For the displacement along the boundary of a hybrid element, we introduce the standard quadratic interpolation function $\mathbf{L}$ to ensure proper matching

with boundary displacement of the adjacent eight node iso-parametric non-singular element as follows:

$$\bar{\mathbf{U}} = \mathbf{L}\mathbf{q} \tag{5}$$

where $\mathbf{q}$ is the nodal degrees of freedom common to the hybrid element and the surrounding regular elements. Substitution of eqns (4) and (5) into eqn (3) yields

$$\pi_{mh} = -\tfrac{1}{2}\boldsymbol{\beta}^T\mathbf{H}\boldsymbol{\beta} + \boldsymbol{\beta}^T\mathbf{G}\mathbf{q} - \boldsymbol{\beta}^T\mathbf{I} + \mathbf{J}\mathbf{q} + C_0, \tag{6}$$

where

$$\mathbf{H} = \frac{1}{2}\int_{\partial A_m} (\mathbf{R}^T\underline{\mathbf{U}} + \underline{\mathbf{U}}^T\mathbf{R})\,\mathrm{d}s, \quad \mathbf{G} = \int_{\partial A_m} \mathbf{R}^T\mathbf{L}\,\mathrm{d}s, \quad \mathbf{J} = \int_{\partial A_m} \mathbf{T}^{pT}\mathbf{L}\,\mathrm{d}s,$$

$$\mathbf{I} = \frac{1}{2}\left[\int_{\partial A_m} \mathbf{R}^T\mathbf{U}^p\,\mathrm{d}s + \int_{\partial A_m} \underline{\mathbf{U}}^T\mathbf{T}^p\,\mathrm{d}s - \iint_{A_m} \mathbf{P}^T\boldsymbol{\varepsilon}^A\,\mathrm{d}A\right],$$

$$C_0 = -\frac{1}{2}\left[\int_{\partial A_m} \mathbf{T}^{pT}\mathbf{U}^p\,\mathrm{d}s - \iint_{A_m} \boldsymbol{\sigma}^{pT}\boldsymbol{\varepsilon}^A\,\mathrm{d}A\right].$$

Taking a variation of π_{mh} with respect to $\boldsymbol{\beta}$ and $\mathbf{q}$, one obtains the stiffness matrix $\mathbf{k}_s$ and the loading vector as

$$\mathbf{k}_s = \mathbf{G}^T\mathbf{H}^{-1}\mathbf{G}, \quad \mathbf{Q}_s = \mathbf{G}^T\mathbf{H}^{-1}\mathbf{I} - \mathbf{J}^T, \tag{7a,b}$$

with

$$\boldsymbol{\beta} = \mathbf{H}^{-1}(\mathbf{G}\mathbf{q} - \mathbf{I}).$$

3.2. *Solution procedure*

The remaining elements surrounding the hybrid element are formulated on the basis of the generalized plane deformation theory and the minimum potential energy principle. Because there is no singularity involved, formulation of the displacement based conventional element is relatively simple. An iso-parametric element with eight nodes and three degrees of freedom per node is used to model the regular elements. Derivation of the stiffness matrix $\mathbf{k}_r$ and the load vector $\mathbf{Q}_r$ for the regular elements is described in Chan and Ochoa (1990).

The summation of the two types of element stiffness all over the elements will yield the global stiffness $\hat{\mathbf{K}}$, and the global load vector $\hat{\mathbf{Q}}$ may be assembled. Symbolically we may express the assemblage process as

$$\hat{\mathbf{K}} = \sum_M \mathbf{k}_r + \mathbf{k}_s, \quad \hat{\mathbf{Q}} = \sum_M \mathbf{Q}_r + \mathbf{Q}_s, \tag{8a,b}$$

where M indicates the total number of the regular elements. Imposing the appropriate displacement boundary conditions, the final form of equilibrium equations may be written in the matrix form

$$\mathbf{K}\mathbf{q} = \mathbf{Q}, \tag{9}$$

where $\mathbf{K}$ is now symmetric and positive definite, so that we can solve eqn (9) for the unknown nodal displacements.

As discussed earlier, the crack faces may be in partial contact with each other depending upon the geometry and end loadings and the contact area is not known *a priori*. To treat such a contact problem, we consider the following quadratic problem.

$$\text{Minimize} \quad \tfrac{1}{2}\mathbf{q}^T\mathbf{K}\mathbf{q}-\mathbf{Q}^T\mathbf{q}$$
$$\text{subject to} \quad \mathbf{A}\mathbf{q} \leqslant 0. \tag{10}$$

Here, at a contact point of crack faces, the impenetrability condition is given by the inequality constraint $\mathbf{Aq} \leqslant 0$ where $\mathbf{Aq}$ represents a difference of a nodal displacement at presumable contact points. We now develop an alternative form of Lagrangian dual problem of maximizing $\theta(\lambda)$ over $\lambda \geqslant 0$, where

$$\theta(\lambda) = \min_{\mathbf{q}}[\tfrac{1}{2}\mathbf{q}^T\mathbf{K}\mathbf{q}-\mathbf{Q}^T\mathbf{q}+\boldsymbol{\lambda}^T\mathbf{A}\mathbf{q}]. \tag{11}$$

Note that for a given λ, the function $\frac{1}{2}\mathbf{q}^T\mathbf{K}\mathbf{q}-\mathbf{Q}^T\mathbf{q}+\boldsymbol{\lambda}^T\mathbf{A}\mathbf{q}$ is strictly convex and achieves its minimum at a point satisfying

$$\mathbf{K}\mathbf{q}-\mathbf{Q}+\mathbf{A}^T\boldsymbol{\lambda} = 0. \tag{12}$$

Substituting eqn (12) into eqn (11), we obtain

$$\theta(\lambda) = -\tfrac{1}{2}\boldsymbol{\lambda}^T\mathbf{D}\boldsymbol{\lambda}-\mathbf{F}^T\boldsymbol{\lambda},$$

where $\mathbf{D} = \mathbf{A}\mathbf{K}^{-1}\mathbf{A}^T$, and $\mathbf{F} = -\mathbf{A}\mathbf{K}^{-1}\mathbf{Q}$. The standard dual problem is thus given by

$$\text{Minimize} \quad \theta(\lambda) = \tfrac{1}{2}\boldsymbol{\lambda}^T\mathbf{D}\boldsymbol{\lambda}+\mathbf{F}^T\boldsymbol{\lambda}$$
$$\text{subject to} \quad \boldsymbol{\lambda} \geqslant 0. \tag{13}$$

Then using Lemke's algorithm (Lemke, 1968), we can solve the above standard quadratic problem efficiently. After λ is obtained through the algorithm, the nodal displacements $\mathbf{q}$ and free constants $\boldsymbol{\beta}$ in the asymptotic representation are then determined, which will complete the solution.

3.3. *Solution in terms of loading parameters*

As discussed earlier, it is rather meaningless to give the solution in terms of deformation parameters $A_i (i = 1\text{–}4)$ in the presence of elastic coupling among extension, bending and/or torsion; for the loadings are in general prescribed in terms of the end loads or the loading parameters not in terms of the deformation parameters. To convert the solution in terms of the deformation parameters into the solution in terms of the end loadings—axial force, bending moment and/or twisting moment, we impose the traction conditions in terms of the resultants on the end cross section. These conditions for a laminated composite strip under the aforementioned generic loadings are written as:

$$\iint_B \sigma_{13}\,dx_1\,dx_2 = 0, \tag{14a}$$

$$\iint_B \sigma_{23}\,dx_1\,dx_2 = 0, \tag{14b}$$

$$\iint_B \sigma_{33}\,dx_1\,dx_2 = P_3, \tag{14c}$$

$$\iint_B \sigma_{33}x_1\,dx_1\,dx_2 = M_2, \tag{14d}$$

$$\iint_B \sigma_{33}x_2\,dx_1\,dx_2 = M_1, \tag{14e}$$

$$\int\int_B (\sigma_{23}x_1 - \sigma_{13}x_2)\,dx_1\,dx_2 = M_t, \tag{14f}$$

where the integrals are taken over the entire area of the cross section, and P_3, M_1, M_2 and M_t are the applied uniaxial tension or compression, pure bending moments and twisting moment acting on the cross section of strip, respectively. Since the left hand side of eqns (14a–f) may be expressed in terms of a linear combination of the deformation parameters (A_1, A_2, A_3 and A_4), eqns (14c–f) can be rewritten as follows:

$$\begin{bmatrix} \Gamma_{11} & \Gamma_{12} & \Gamma_{13} & \Gamma_{14} \\ \Gamma_{21} & \Gamma_{22} & \Gamma_{23} & \Gamma_{24} \\ \Gamma_{31} & \Gamma_{32} & \Gamma_{33} & \Gamma_{34} \\ \Gamma_{41} & \Gamma_{42} & \Gamma_{43} & \Gamma_{44} \end{bmatrix} \begin{bmatrix} A_1 \\ A_2 \\ A_3 \\ A_4 \end{bmatrix} = \begin{bmatrix} P_3 \\ M_2 \\ M_1 \\ M_t \end{bmatrix} \quad \text{with} \quad \Gamma_{ij} = \Gamma_{ji}. \tag{15}$$

4. NUMERICAL RESULTS AND DISCUSSION

In this section, two examples of wedge problems, free edge problems and delamination problems for laminated composite strips, are given for laminated composite strips subjected to generic loadings of generalized plane deformation. For numerical computation, we use the same material data as in Part I (Kim and Im, 1994).

4.1. *Free edge problem under generalized plane deformation*

The free edge problem is first chosen to illustrate the application of the singular hybrid finite element method to a laminated composite strip subjected to the aforementioned generic loadings (Fig. 1).

The singular nature of the stress field near the free edge was discussed by Wang and Choi (1982), and Zwiers *et al.* (1982). In Part I (Kim and Im, 1994), it has been shown that there exists a single scaling parameter governing the free edge singular field. We here define

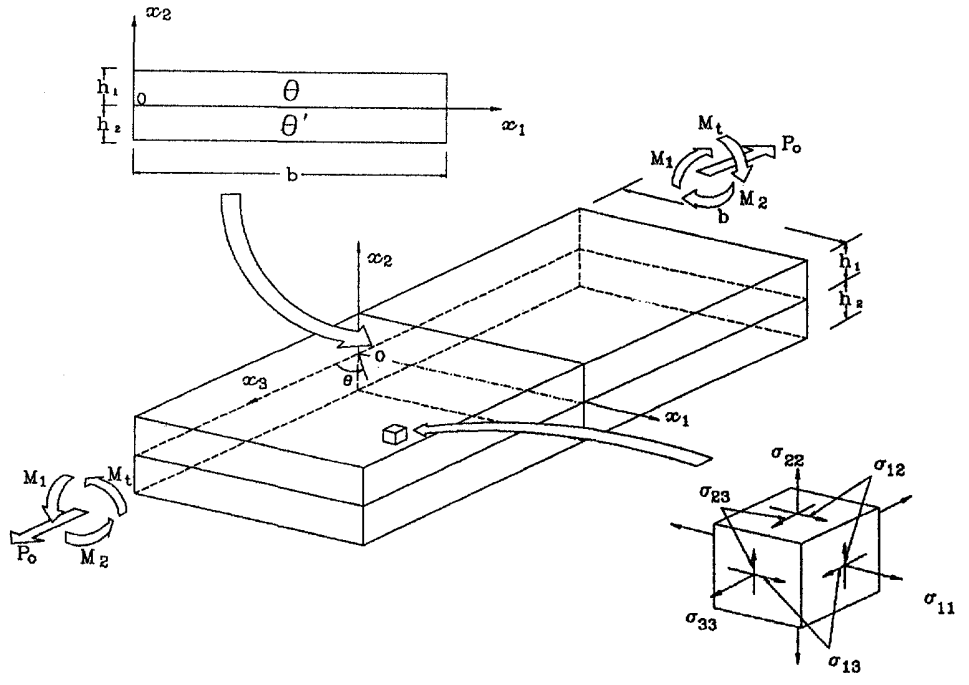

Fig. 1. Free edge problem under generic loadings of generalized plane deformation such as tension, bending and torsion.

the single scaling parameter to be the so called "free edge stress intensity", and introduce the "mode vector" to describe all of singular stress components near the free edge. These parameters will be interpreted from the viewpoint of fracture mechanics, particularly in association with the initiation of delamination cracks from the free edge. The numerical examples will be given for varying ratio of ply thickness, and we will confirm the convergence of the present singular hybrid FEM on the basis of the numerical results.

Following Kim and Im (1994), the singular stress field near the free edge can be written as

$$\sigma_{ij}^{s}(r,0) = \frac{K_r r^{\delta_1^s}}{\sqrt{2\pi}} \omega_{ij}, \tag{16}$$

where

$$\omega_{ij} = \mathrm{Re}\left(\sum_{k=1}^{3} b_{ks}\tau_{ijk}\right), \quad K_r = \sqrt{2\pi}\gamma_{3s} \quad (ij = 11, 22, 33, 23, 31, 21).$$

Among the most important failure or fracture modes for the free edge is the delamination, which will be governed by the asymptotic singular traction vector on the interfacial plane near the free edge. This traction vector is determined by K_r and ω_{ij}. That is, let $\mathbf{t}^s$ denote the singular traction vector on the interfacial plane. Then,

$$\mathbf{t}^s(r,0) = [\sigma_{21}, \sigma_{22}, \sigma_{23}]^T = \frac{K_r r^{\delta_1^s}}{\sqrt{2\pi}} \boldsymbol{\Omega} \quad (\Omega_1 = \omega_{21}, \Omega_2 = \omega_{22}, \Omega_3 = \omega_{23}). \tag{17}$$

We now name K_r and $\boldsymbol{\Omega}$ the free edge stress intensity and the associated mode vector, respectively, in that K_r governs the delamination behaviour for a given pair of adjacent plies on the free edge, and that $\boldsymbol{\Omega}$ determines the mode mixity of the singular interfacial traction $\mathbf{t}^s$. This equation shows that the interfacial singular traction vector near the free edge is completely expressed in terms of the order of singularity δ_1^s, the scaling parameter K_r and the mode vector $\boldsymbol{\Omega}$. We emphasize that only the free edge stress intensity K_r is dependent upon the far field loading at the remote boundary, while δ_l^s and Ω_i are not dependent upon the far field loading, but solely determined from the elastic properties of the adjacent materials and the near field conditions. However, the definition of K_r varies according to the way of normalizing the mode vector $\boldsymbol{\Omega}$. We here propose one normalization such that $\boldsymbol{\Omega} = [*, 1, *]$ where "*" signifies numbers determined via the eigenvalue problem obtained from the near field conditions. Note that this normalization is invalid when $\sigma_{22} = 0$.

The fact that the single parameter K_r characterizes the near tip field for any far field loading is an important implication in association with the prediction of delamination failure near the free edge; i.e. we do material testing to determine a critical value of K_r, for example, the value of K_r^c for initiation of delamination, under a simple loading such as uniaxial tension. Then this critical value is a material constant, which is applicable to assessing any real structure of the same materials under a real complex loading. For fatigue loading, the initiation of delamination crack may be governed by a total number of cycles for a given change of the free edge stress intensity ΔK_r, and an average value of K_r during one cycle. In passing, we remark that such an observation cannot be made via the six boundary layer stress intensities defined by Wang and Choi (1982).

In constructing the singular hybrid finite element, the entire area of cross-section is modelled because there are no symmetry in geometry and lamination. The composite has the geometry of $b/h = 4$ and $h_1 = h_2 = 0.125$ mm with $h = h_1 + h_2$ (see Fig. 2 or the figures on the top of Tables 1–5). A typical finite element mesh configuration is shown in Fig. 2, wherein the region is discretized by the conventional iso-parametric element with 58 elements and 209 nodes, and by one singular hybrid element with 9 nodes.

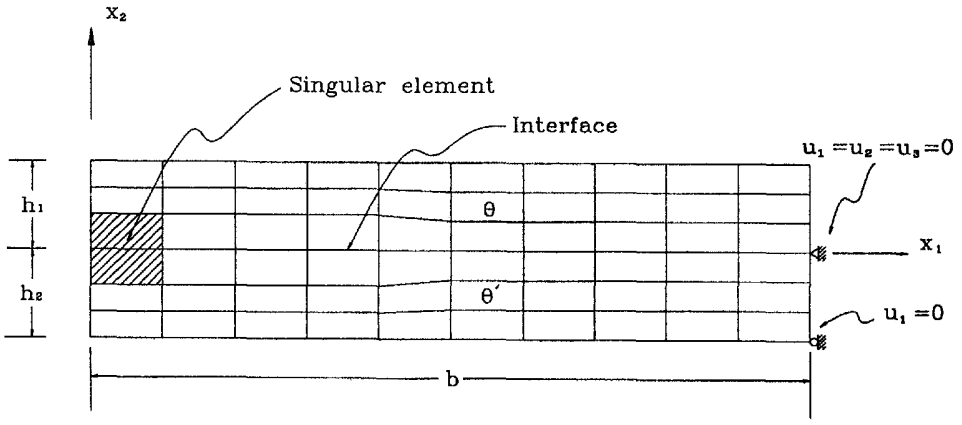

Fig. 2. Typical finite element mesh configuration for free edge problem in $[\theta/\theta']$ composite laminates.

When the generic loadings such as uniaxial tension or compression, pure bending and/or torsion are applied in $[\theta/\theta']$ composite laminates, the relation (15) between the generic loadings and the deformation parameters is obtained from the conditions (14a–f) on the cross-sectional area. Numerical results for stiffness matrix Γ_{ij} of eqn (15) obtained via the singular hybrid FEM, are tabulated for $[\theta/\theta']$ composite laminates in Table 1. As expected, the stiffness matrix Γ_{ij} is symmetric and its components Γ_{13}, Γ_{23} and Γ_{34} are equal to zero for $[\theta/-\theta]$ composite laminates. These results can be confirmed through the classical lamination theory. The difference in numerical results of Γ_{ij} is just a few percentage between the present hybrid FEM and the classical lamination theory, which shows that the classical lamination theory is accurate enough as far as the overall stiffness of a composite laminate is concerned.

The convergence of the singular hybrid FEM with the number of eigenvalues is shown in terms of K_r normalized by each loading in Table 2, and the present solution has a very

Table 1. Stiffness matrix Γ_{ij} for the free edge in composite laminates subjected to tension, bending and torsion

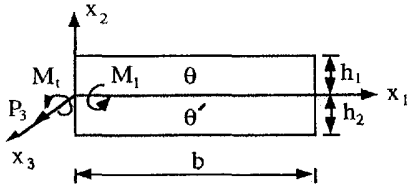

$(h = h_1 + h_2,\ h/b = 0.25,\ h_1/h_2 = 1,\ b = 1\ \text{mm})$

	$[\theta/\theta']$			
Γ_{ij}	[30/−45]	[45/−45]	[60/−45]	[60/−60]
Γ_{11}	7.1004	4.5243	3.5897	2.9358
Γ_{12}	3.5502	2.2621	1.7948	1.4679
Γ_{13}	0.1165	0	−0.0303	0
Γ_{14}	−0.2944	−0.1743	−0.1025	−0.0514
Γ_{22}	2.2905	1.4785	1.1849	0.9753
Γ_{23}	0.0582	0	−0.0151	0
Γ_{24}	−0.1472	−0.0871	−0.0512	−0.0257
Γ_{33}	0.0315	0.0210	0.0185	0.0150
Γ_{34}	−0.0107	0	0.0067	0
Γ_{44}	0.0651	0.0634	0.0540	0.0463

Table 2. Solution convergence versus the number of eigenvalues in terms of the free edge stress intensity in $[\theta/\theta']$ composite laminates

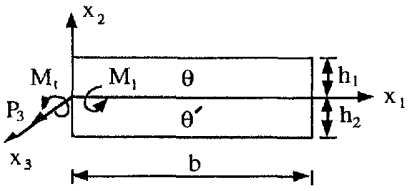

($h = h_1 + h_2$, $h/b = 0.25$, $h_1/h_2 = 1$, $b = 1$ mm)

Loading	N	$[\theta/\theta']$ [45/−45]	[60/−60]	[30/−45]	[60/−45]
Tension K_r/P_3 unit: $mm^{\delta'_1} mm^{-2}$	11	−19.0503	−11.5644	−16.9758	−11.9438
	15	−18.9727	−11.5622	−17.1205	−9.6842
	19	−18.9369	−11.5629	−17.1271	−9.6513
	23	−18.9408	−11.5616	−17.1328	−9.6440
Bending K_r/M_1 unit: $mm^{\delta'_1} mm^{-3}$	11	−0.1098	−0.0346	5.6663	−6.7581
	15	−0.0131	−0.0007	7.2247	−5.6956
	19	−0.0004	0	8.4321	−4.8667
	23	0	0	8.4404	−4.8453
Torsion K_r/M_t unit: $mm^{\delta_1} mm^{-3}$	11	−33.0158	−35.3644	−38.8138	−22.7126
	15	−35.0563	−35.1090	−36.9184	−28.4191
	19	−35.5760	−35.1439	−37.1287	−28.8146
	23	−35.5272	−35.1332	−37.2488	−28.8211

N, the number of eigenvalues.

stable convergence characteristic. In this table, note that the free edge stress intensity K_r has the value of 0 for $[\theta/-\theta]$ composite laminates subjected to pure bending about the x_1-axis because the interface ($x_2 = 0$) becomes the neutral plane and does not undergo any axial stretching under pure bending. Failure to include the logarithmic term $z_k \ln z_k$, which appears under torsion in the eigenfunction series, will seriously degrade the accuracy of the

Table 3. Stiffness matrix Γ_{ij} in delaminated $[\theta/\theta']$ composite laminates subjected to tension, bending and torsion

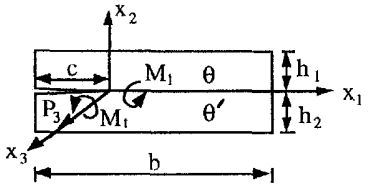

($h = h_1 + h_2$, $h/b = 0.25$, $c/b = 0.125$, $h_1/h_2 = 1$, $b = 1$ mm)

Γ_{ij}	$[\theta/\theta']$ [30/−45]	[45/−45]	[60/−45]	[60/−60]
Γ_{11}	6.7732	4.3940	3.5358	2.9202
Γ_{12}	2.6513	1.6926	1.3448	1.1006
Γ_{13}	0.1112	0	−0.0294	0
Γ_{14}	−0.2607	−0.1543	−0.0908	−0.0455
Γ_{22}	1.5130	0.9833	0.7922	0.6542
Γ_{23}	0.0435	0	−0.0113	0
Γ_{24}	−0.1090	−0.0646	−0.0380	−0.0191
Γ_{33}	0.0313	0.0209	0.0184	0.0149
Γ_{34}	−0.0102	0	0.0065	0
Γ_{44}	0.0615	0.0603	0.0514	0.0440

Table 4. Solution convergence versus the number of eigenvalues in terms of the stress intensity factors in delaminated $[\theta/\theta']$ composite laminates

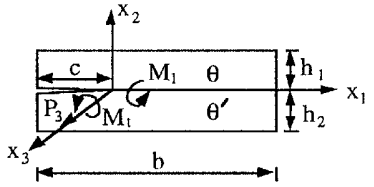

($h = h_1 + h_2$, $h/b = 0.25$, $c/b = 0.125$, $h_1/h_2 = 1$, $b = 1$ mm)

		$[\theta/\theta']$					
		[45/−45]			[60/−45]		
Loading	N	K_1/R	K_2/R	K_3/R	K_1/R	K_2/R	K_3/R
Tension $R = P_3$ unit: $mm^{-3/2}$	6	0.8870	2.8140	0.0094	0.7751	2.0129	0.4882
	9	1.2292	2.9436	0.0203	1.1493	2.0488	0.5385
	14	1.5379	2.9885	0.0229	1.4975	2.1057	0.5452
	19	1.5558	2.9880	0.0239	1.5333	2.1011	0.5429
Bending $R = M_1$ unit: $mm^{-5/2}$	6	0	0	−4.4049	0.3448	6.2331	−1.6822
	9	0	0	−4.8065	0.4118	6.6367	−1.9943
	14	0	0	−4.8245	0.4947	6.7025	−2.0260
	19	0	0	−4.8261	0.5086	6.7241	−2.0456
Torsion $R = M_t$ unit: $mm^{-5/2}$	6	3.2487	−15.016	0.6973	3.3784	−15.487	−4.3350
	9	3.6909	−14.830	0.6923	3.6826	−15.356	−4.2235
	14	3.8728	−14.775	0.6876	3.9251	−15.406	−4.1389
	19	3.8450	−14.767	0.6854	3.9135	−15.477	−4.0762

N, the number of eigenvalues.

numerical results in the present hybrid FEM because this will invalidate the asymptotic solution via violating the near field conditions.

To investigate the influence of laminate geometric variables for the free edge problem, we compute the free edge stress intensity K_r for various ply thickness. For $[\theta/\theta']$ composite laminates under various loadings, the free edge stress intensity K_r is plotted versus the

Table 5. Comparison of two crack tip models in [45/−45] composite laminates subjected to pure bending about the x_1-axis

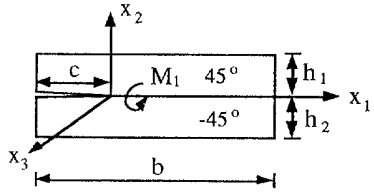

($h = h_1 + h_2$, $h/b = 0.25$, $c/b = 0.125$, $h_1/h_2 = 1$, $b = 1$ mm)

	Two models							
	Opened crack tip model				Closed crack tip model			
N	K_1/M_1 ($mm^{-5/2}$)	K_2/M_1 ($mm^{-5/2}$)	K_3/M_1 ($mm^{-5/2}$)	G/M_1 (mm^{-2})	K_1/M_1 ($mm^{-5/2}$)	K_{II}/M_1 ($mm^{-5/2}$)	K_{III}/M_1 ($mm^{-5/2}$)	G/M_1 (mm^{-2})
6	0	0	−4.4049	1.2194	0	−4.4145	0	1.2248
9	0	0	−4.8065	1.4519	0	−4.8065	0	1.4519
14	0	0	−4.8245	1.4628	0	−4.8244	0	1.4628
19	0	0	−4.8261	1.4638	0	−4.8263	0	1.4639

N, the number of eigenvalues.

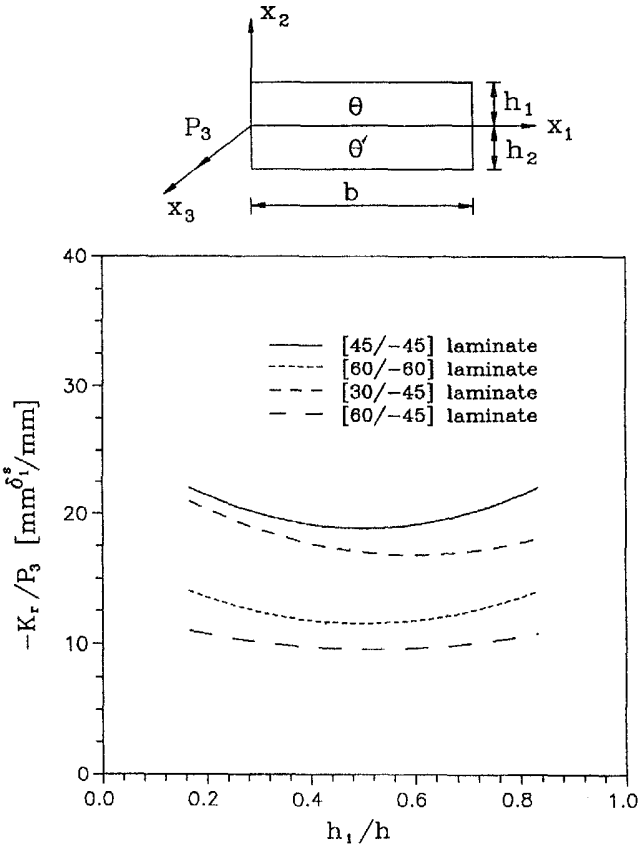

Fig. 3. The free edge stress intensity versus the relative ply thickness for the free edge problem under tension along the x_3-axis ($h = h_1 + h_2 = 0.25$ mm: fixed).

relative ply thickness h_1/h in Figs 3–5 (with $h = h_1 + h_2$ and b fixed). As shown in Figs 3 and 4, the free edge stress intensity $|K_r|$ has a minimum value under tension at the near $h_1/h = 1/2$, On the other hand, $|K_r|$ for bending about the x_1-axis is linearly proportional to h_1/h, and $|K_r|$ under torsion along the x_3-axis has a maximum value at the near $h_1/h = 1/2$. This is consistent with the fact that the bending strain is linearly proportional to the distance from the neutral axis and the shear strain under torsion increases for a prismatic bar with a rectangular cross-section as we proceed from the vertex of a rectangle to the middle of an edge on the cross-section.

4.2. *Delamination crack problem under generalized plane deformation*

The delamination crack problem is selected as another example for the boundary layer region of a wedge type cross-section of a laminated composite strip subjected to the aforementioned generic loadings (Fig. 6). Through this example, the convergence of numerical solution will be confirmed in terms of stress intensity factors defined by Suo (1990), and the energy release rate will be given for varying ratios of relative ply thickness.

The eigenvalues for a delamination crack are given, according to crack face conditions, as (Kim and Im, 1993)

$$n-\tfrac{1}{2} \pm i\eta \text{ and } n \quad \text{for the opened crack,}$$

$$n-\tfrac{1}{2} \text{ and } n \quad \text{for the closed crack.}$$

One of the two eigensolutions either for an opened crack or for a closed crack needs to be chosen for constructing the singular hybrid crack tip element. In general, however, we do not know *a priori* whether the crack tip is opened or closed. To know the exact crack face

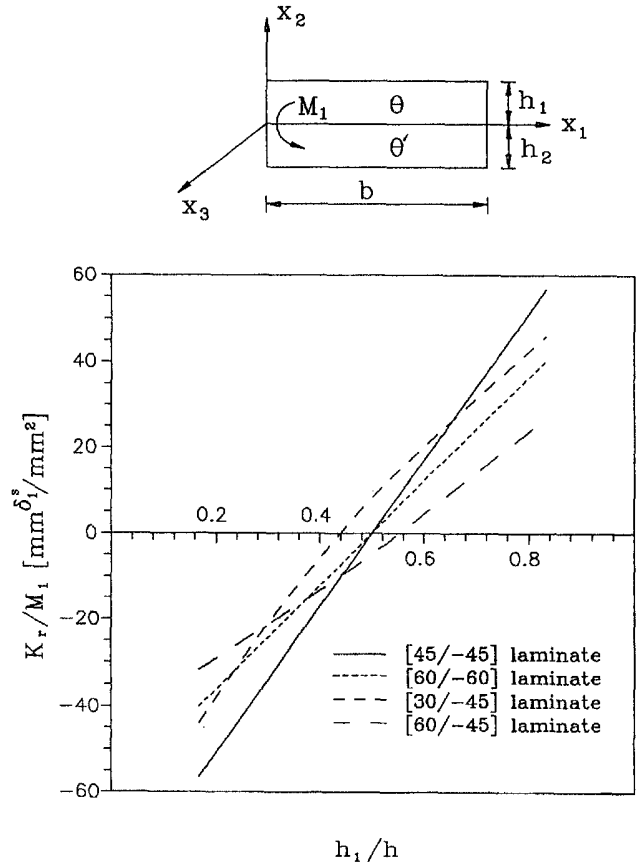

Fig. 4. The free edge stress intensity versus the relative ply thickness for the free edge problem under pure bending about the x_1-axis ($h = h_1 + h_2 = 0.25$ mm : fixed).

behaviour, we first perform the regular finite element analysis with fine mesh, and based upon the regular FEM results we choose one of the two asymptotic solutions.

In an opened delamination crack, the near tip traction $\mathbf{t}^s(r,0) = [\sigma_{21}, \sigma_{22}, \sigma_{23}]^T$ on the interface can be written as (see Appendix for details)

$$\mathbf{t}^s(r,0) = \frac{1}{\sqrt{2\pi r}}[Kr^{i\eta}\mathbf{w} + \bar{K}r^{-i\eta}\bar{\mathbf{w}} + K_3\mathbf{w}^0].$$

As pointed out by Suo (1990), there are three real scaling parameters (one complex stress intensity factor K and one real stress intensity factor K_3) characterizing the near tip field of an interfacial crack. However, the complex intensity factor K has the length scale dependency, and we therefore use the following stress intensity factors K_1 and K_2, as suggested by Rice (1988), at a specific reference length $\hat{r}$,

$$\mathbf{t}^s(r,0) = \frac{1}{\sqrt{2\pi r}}[(K_1 + iK_2)(r/\hat{r})^{i\eta}\mathbf{w} + (K_1 - iK_2)(r/\hat{r})^{-i\eta}\bar{\mathbf{w}} + K_3\mathbf{w}^0]. \tag{18}$$

For the present case, we take $\hat{r}$ to be $c/50$. Because the imaginary part of singularity η is very small ($0.01 < \eta < 0.02$), changing the value of $\hat{r}$ within a modest range, say, an order of a factor of 10 or less, does not affect the values of K_1 and K_2 significantly (Rice, 1988).

For numerical examples, we take the same geometric dimension as in the free edge problem: $b/h = 4$ and $h_1 = h_2 = 0.125$ mm with $h = h_1 + h_2$. We assume no symmetry in geometry and lamination (Fig. 6). A typical mesh configuration for regular finite element method is shown in Fig. 7. From numerical results obtained by employing the eight-node,

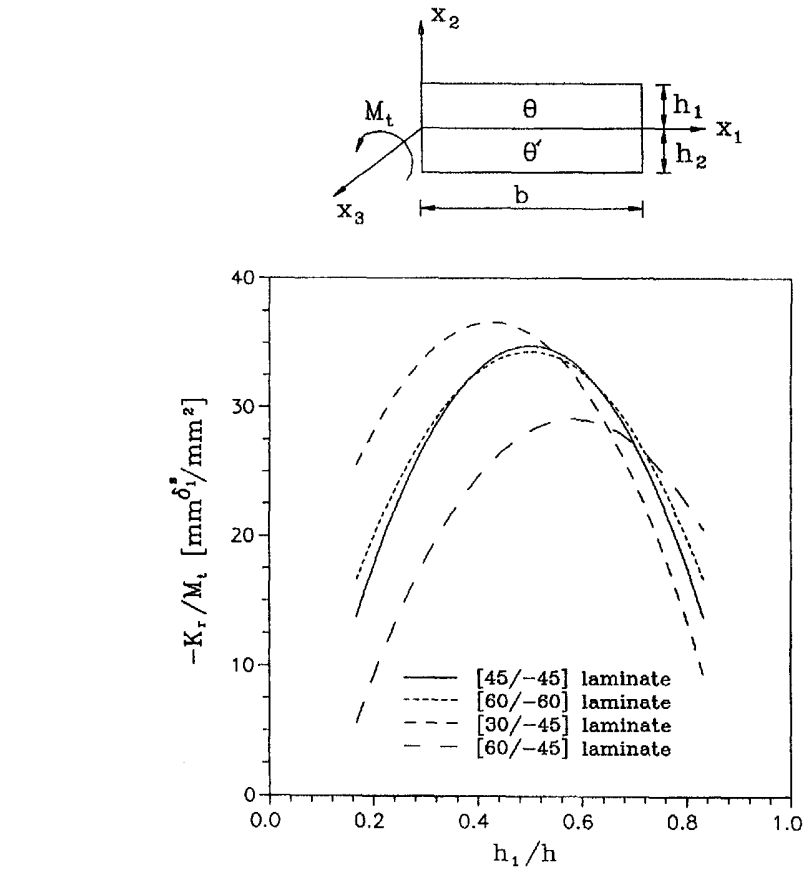

Fig. 5. The free edge stress intensity versus the relative ply thickness for the free edge problem under torsion along the x_3-axis ($h = h_1 + h_2 = 0.25$ mm: fixed).

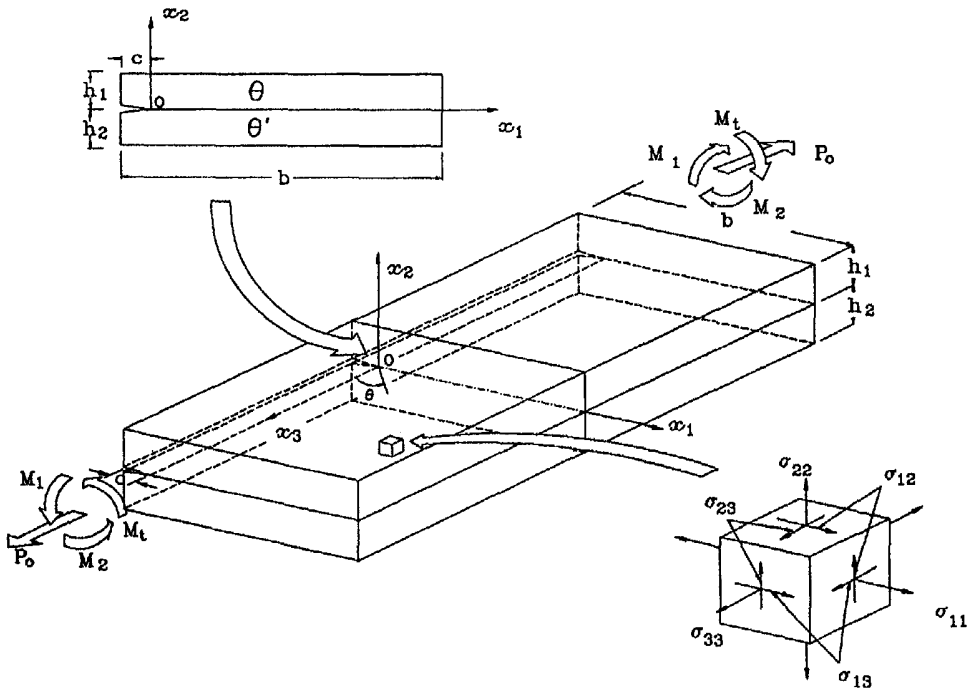

Fig. 6. Delamination problem under generic loadings of generalized plane deformation such as tension, bending and torsion.

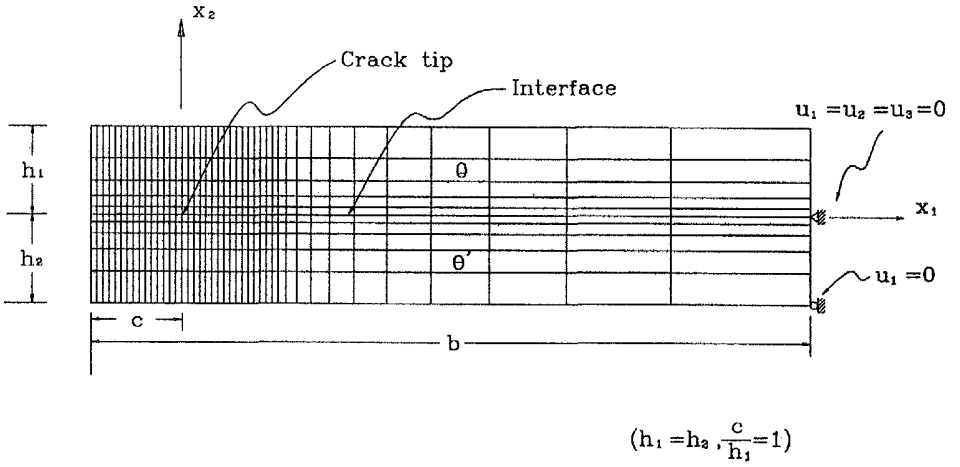

Fig. 7. Mesh configuration for regular finite element method in delaminated $[\theta/\theta']$ composite laminates.

conventional iso-parametric elements (Fig. 7) with 470 and 1555 nodes, the crack tip is found to be opened for all cases of the present numerical computation except for $[\theta/-\theta]$ composite laminates with $h_1/h = 1/2$ under pure bending about the x_1-axis: it turns out that these $[\theta/-\theta]$ composite laminates are satisfied for both opened crack tip condition and closed crack tip condition. When $h_1/h \neq 1/2$, however, the crack tip turns out to be opened. This result is consistent with the fact that the interfacial plane is corresponding to the neutral plane under pure bending about the x_1-axis when $h_1/h = 1/2$. On the other hand, crack faces apart from the crack tip may be opened or closed depending upon loading, geometry and lamination sequence. On the basis of these observations, the singular hybrid finite element method with a combination of the singular element having the asymptotic solutions for an opened crack and nonsingular iso-parametric elements (Fig. 8), 135 elements and 467 nodes, is then used to examine the boundary layer region in detail.

To obtain relations between the generic loadings and the deformation parameters, the stiffness matrix Γ_{ij} is computed in Table 3. Comparing the stiffness matrix Γ_{ij} for the free edge in Table 1 with those for the delamination crack problem in Table 3, we see that there occurs stiffness reduction due to the existence of a crack.

To confirm the convergence of the numerical solution, we compute the stress intensity factors varying the number of the eigenvalues. The convergence of the numerical solutions is confirmed as shown in Table 4. For the $[\theta/-\theta]$ composite laminates satisfying both of the opened crack tip condition and the closed crack tip condition under pure bending about

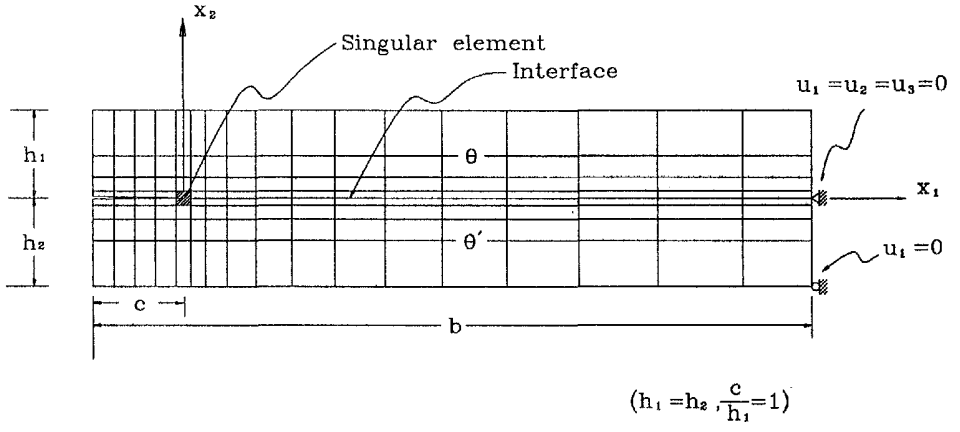

Fig. 8. Mesh configuration for singular hybrid finite element method in delaminated $[\theta/\theta']$ composites laminates.

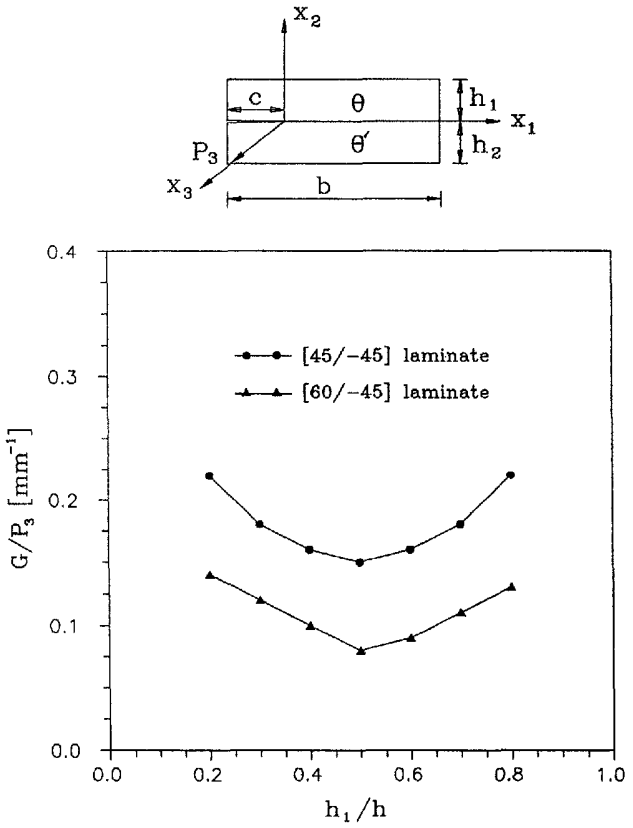

Fig. 9. Energy release rate versus the relative ply thickness in a delaminated composite strip subjected to tension along the x_3-axis ($h = h_1 + h_2 = 0.25$ mm: fixed).

the x_1-axis, comparison of two models is made in Table 5. The solutions for two different crack tip models show an excellent agreement. Note that the complex part $K_1 + iK_2$ of the stress intensity, which is associated with the oscillatory near tip mode, vanishes in the eqn (18) for the opened crack model, and only the real part K_3 of the stress intensity exists, which yields only the mode II for this case. In Figs 9 and 10, the energy release rate is calculated versus the relative ply thickness in $[\theta/\theta']$ composite laminates subjected to tension and bending about the x_1-axis, and the minimum energy release rate is obtained at the near $h_1/h = 1/2$, which may be expected for the case of pure bending. The results for tension in this case shows the similar behaviour as in the case of the free edge problem compared with Fig. 3.

5. CONCLUSION

The complete solutions under generalized plane deformation in composite laminates subjected to uniaxial tension/compression, pure bending and/or torsion are obtained with the aid of the singular hybrid finite element method combined with the asymptotic solutions given in Kim and Im (1994). The free edge problem and the delamination crack problem are given as numerical examples. Numerical results for two examples are summarized as follows:

(1) The present numerical scheme shows an excellent convergence behaviour with respect to the number of eigenfunction terms incorporated.
(2) The free edge stress intensity K_r governs the fracture behaviour or failure behaviour for a given pair of adjacent plies, such as the initiation of delamination near the free edge, regardless of loadings, once a proper normalization for the mode vector is chosen.

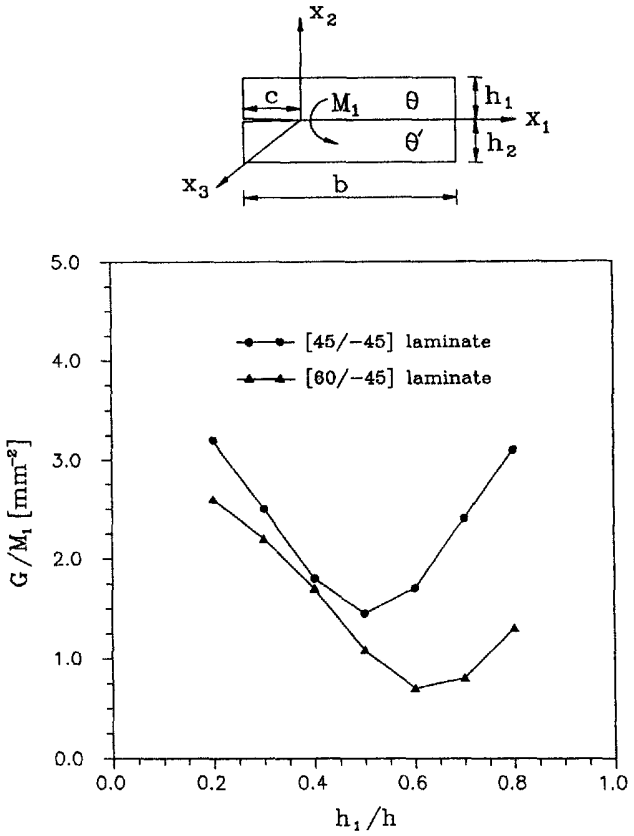

Fig. 10. Energy release rate versus the relative ply thickness in a delaminated composite strip subjected to pure bending about the x_1-axis ($h = h_1 + h_2 = 0.25$ mm: fixed).

(3) The delamination crack tip is found to be opened for all cases of the present numerical computation. Particularly, for the $[\theta/-\theta]$ composite laminates subjected to pure bending about the x_1-axis, the oscillatory part of the singular traction on the interface vanishes and only the shear traction exists, so that this case satisfies the conditions for the two models (the opened crack tip model and the closed crack tip model), and numerical results for the two models show an excellent agreement.

Acknowledgement—The present work has been supported by the Agency for Defence Development (ADD) under the Grant No. ADD-92-5-004. This grant is gratefully acknowledged.

REFERENCES

Atluri, S. N. and Nakagaki, M. (1986). Computational methods for plane problems of fracture. In *Computational Methods in Mechanics of Fracture* (Edited by S. N. Atluri), pp. 169–227. Elsevier, Amsterdam.

Chan, W. S. and Ochoa, O. O. (1990). Delamination characterization of laminates. *Computational Mech.* **6,** 393–403.

Kim, T. W. and Im, S. (1991). Delamination crack originating from transverse cracking in cross-ply composite laminates under extension. *Int. J. Solids Structures* **27,** 1925–1941.

Kim, Y. and Im, S. (1993). Delamination cracks originating from transverse cracking in cross-ply laminates under various loadings. *Int. J. Solids Structures* **30,** 2143–2161.

Kim, T. W. and Im, S. (1994). Boundary layers in wedges of laminated composite strips under generalized plane deformation—part I: asymptotic solutions. *Int. J. Solids Structures* **32,** 609–628.

Lemke, C. E. (1968). On complementary pivot theory. In *Mathematics of the Decision Sciences* (Edited by G. B. Dantzig and A. F. Veinott), pp. 95–114. American Mathematical Society, New York.

Rice, J. R. (1988). Elastic fracture mechanics concepts for interfacial cracks. *ASME J. Appl. Mech.* **55,** 98–103.

Stolarski, H. K. and Chiang, M. Y. M. (1989). On the significance of the logarithmic term in the free edge stress singularity of composite laminates. *Int. J. Solids Structures.* **25,** 75–93.

Suo, Z. (1990). Singularities, interfaces and cracks in dissimilar anisotropic media. *Proc. R. Soc Lond. A* **427,** 331–358.

Wang, S. S. (1984). Edge delamination in angle-ply composite laminates. *AIAA J.* **22,** 256–264.
Wang, S. S. and Choi, I. (1982). Boundary-layer effect in composite laminates, part I—free-edge stress singularities; part II—free-edge stress solutions and characteristics. *ASME J. Appl. Mech.* **49,** 541–550.
Wang, S. S. and Yuan, F. G. (1983). A hybrid finite element approach to composite laminates elasticity problems with singularities. *ASME J. Appl. Mech.* **50,** 835–844.
Washizu, K. (1988). Variational methods in elasticity and plasticity. 3rd Edition, Pergamon Press, Oxford, U.K.
Zwiers, R. I., Ting, T. C. T. and Spilker, R. L. (1982). On the logarithmic singularity of free edge stress in laminated composites under uniform extension. *ASME J. Appl. Mech.* **49,** 562–569.

APPENDIX

Based upon the asymptotic representation at the near tip field, Suo's stress intensity factors for an interfacial crack in anisotropic materials are described here.

Following Kim and Im (1994), we have the near tip traction $\mathbf{t}^s(r, 0) = [\sigma_{21}, \sigma_{22}, \sigma_{23}]^T$ on the interface as

$$\mathbf{t}^s(r, 0) = \frac{1}{\sqrt{2\pi r}}[Kr^{i\eta}\mathbf{w} + \bar{K}r^{-i\eta}\bar{\mathbf{w}} + K_3\mathbf{w}^0],$$

where

$$K = \sqrt{2\pi}(\gamma_{1s} - i\gamma_{2s}), \quad \eta = \mathrm{Im}(\delta_c^s), \quad w_j = \sum_{k=1}^{3}(b_{ks}\tau_{2jk} + b_{(k+3)s}\bar{\tau}_{2jk}),$$

$$w_j^0 = \mathrm{Re}\left(\sum_{k=1}^{3} b_{ks}\tau_{2jk}\right), \quad K_3 = \sqrt{2\pi}\gamma_{3s} \quad (j = 1, 2, 3),$$

and δ_c^s is the complex singular eigenvalue, and $\mathbf{w}$ and $\mathbf{w}^0$ are determined from the following eigenvalue problem obtained from the near field conditions (traction free and continuity conditions)

$$\bar{\mathbf{R}}\mathbf{w} = e^{2\pi\eta}\mathbf{R}\mathbf{w},$$

where

$$R_{ij} = B_{ij} + \bar{B}_{ij},$$

$$B_{ij} = i\sum_{k=1}^{3} H_{ik}L_{kj}^{-1},$$

$$L_{ij} = \sum_{k=1}^{3}(C_{i2k1} + \mu_j C_{i2k2})H_{kj} \quad (i, j = 1, 2, 3).$$

The stress intensity factors K and K_3 become different in accordance with the method of normalizing the eigenvectors $\mathbf{w}$ and $\mathbf{w}^0$. Suo (1990) proposed the following normalization, which recovers the stress intensity factors for isotropic materials:

$$\mathbf{w} = [-i/2, *, *]^T, \quad \mathbf{w}^0 = [*, *, 1]^T,$$

where (*) signifies numbers determined by the eigenvalue problem. He also indicated that this normalization is invalid when $w_1 = 0$ or $\mathbf{w}_3^0 = 0$. In the case of $[\theta/-\theta]$ composite laminates for the given material data in Section 5 of Part I (Kim and Im, 1994), this normalization cannot be used. We thus select a new normalization as follows

$$\mathbf{w} = [*, 1/2, *]^T, \quad \mathbf{w}^0 = [1, *, *]^T.$$

The energy release rate related to the stress intensity factors is given by Suo (1990),

$$G = \frac{\mathbf{w}^T(\mathbf{R} + \bar{\mathbf{R}})\mathbf{w}|K|^2}{4\cosh^2 \pi\eta} + \tfrac{1}{8}\mathbf{w}^{0T}(\mathbf{R} + \bar{\mathbf{R}})\mathbf{w}^0 K_3^2.$$